Development 138, 4661-4671 (2011) doi:10.1242/dev.069161

Drosophila javelin-like encodes a novel microtubule-associated protein and is required for mRNA localization during oogenesis

Dikla Dubin-Bar*, Amir Bitan*, Anna Bakhrat, Simha Amsalem and Uri Abdu†

SUMMARY

Asymmetrical localization of mRNA transcripts during *Drosophila* oogenesis determines the anteroposterior and dorsoventral axes of the *Drosophila* embryo. Correct localization of these mRNAs requires both microtubule (MT) and actin networks. In this study, we have identified a novel gene, CG43162, that regulates mRNA localization during oogenesis and also affects bristle development. We also showed that the *Drosophila* gene *javelin-like,* which was identified based on its bristle phenotype, is an allele of the CG43162 gene. We demonstrated that female mutants for *jvl* produce ventralized eggs owing to the defects in the localization and translation of *gurken* mRNA during mid-oogenesis. Mutations in *jvl* also affect *oskar* and *bicoid* mRNA localization. Analysis of cytoskeleton organization in the mutants reveal defects in both MT and actin networks. We showed that Jvl protein colocalizes with MT network in Schneider cells, in mammalian cells and in the *Drosophila* oocyte. Both in the oocyte and in the bristle cells, the protein localizes to a region where MT minus-ends are enriched. Jvl physically interacts with SpnF and is required for its localization. We found that overexpression of Jvl in the germline affects MT-dependent processes: oocyte growth and oocyte nucleus anchoring. Thus, our results show that we have identified a novel MT-associated protein that affects mRNA localization in the oocyte by regulating MT organization.

KEY WORDS: Gurken, Microtubule, mRNA localization

INTRODUCTION

Asymmetrical mRNA localization in the *Drosophila* oocyte allows the proper localization of axis-determining factors during oogenesis. During mid-oogenesis, *gurken* (*grk*) mRNA is localized around the oocyte nucleus and specifies the dorsal-ventral axis of the oocyte and embryo (Neuman-Silberberg and Schüpbach, 1993; Neuman-Silberberg and Schüpbach, 1996; Ruohola-Baker et al., 1994; Gonzalez-Reyes et al., 1995; Roth et al., 1995). At the same time, *bicoid* (*bcd*) mRNA is localized to the extreme anterior cortex of the oocyte, ultimately leading to a morphogenetic gradient of Bcd protein when it is translated in the embryo (Driever and Nusslein-Volhard, 1988a; Driever and Nusslein-Volhard, 1988b). In addition, *oskar* (*osk*) mRNA is localized to the posterior end of the oocyte and initiates the development of the future germ cells and the abdomen of the embryo (Ephrussi et al., 1991). The asymmetric localization of mRNA within the developing egg chamber during mid-oogenesis relies on the cytoskeleton, and requires both microtubules (MTs) and actin networks, as well as motor proteins. Although the complex organization of MTs and actin during mid-oogenesis has been elucidated, the mechanism that leads to the formation of the specialized MT and actin networks and to the connection between them is still not fully understood.

Previously, we and others have shown that mutations in *spindle-F* (*spn-F*) and in the *Drosophila* IKKε homologue *ik2*, affect both egg chamber polarity and bristle development (Abdu et al., 2006; Shapiro and Anderson, 2006). It has been demonstrated that the defects in egg chamber development in *spn-F* and *ik2* are attributed to their effect on mRNA localization by regulating oocyte cytoskeleton organization. We were also able to show that Ik2 and Spn-F form a complex in which Ik2 phosphorylates Spn-F protein (Dubin-Bar et al., 2008). Beside its role during oogenesis, it has also been demonstrated that *ik2* regulates F-actin assembly by mediating the function of nonapoptotic caspases via degradation of *Drosophila* IAP1 (DIAP1) (Oshima et al., 2006; Kuranaga et al., 2006). Genomic RNAi screens for mitotic genes have revealed that *ik2* plays a role in spindle organization (Bettencourt-Dias et al., 2004; Somma et al., 2008). It has also been suggested that *ik2* regulates dendrite pruning by promoting MT disassembly (Lee et al., 2009) and that mutations in *ik2* affect polarized bristle MT function (Bitan et al., 2010). Recently, a novel role for Ik2 in bristle cell elongation (through regulating recycling endosome shuttling) was suggested (Otani et al., 2011). With regards to their role in cytoskeleton organization, it seems that Ik2 and Spn-F may be involved in either MT or actin organization or in the connections between these two cytoskeleton components.

Using the yeast two-hybrid-based protein-interaction map of the fly proteome along with RNAi in bristles, we identified a novel gene, CG43162, as a possible Spn-F interactor. We have identified several alleles for CG43162. Among them are alleles at the *javelin-like* (*jvl*) locus and we showed that *jvl* has a role both in oogenesis and in bristle development. We have demonstrated that *jvl* mutant females lay eggs with dorsal-ventral defects owing to the defects in the localization and translation of *grk* mRNA. We also observed defects in the localization patterns of *bcd* and *osk* mRNA. We have found that both actin and MT networks are mis-organized in *jvl* mutants and that the Jvl protein colocalizes with MT both in *Drosophila* and mammalian cells. Moreover, we have found that

Department of Life Sciences and the National Institute for Biotechnology in the Negev, Ben-Gurion University, Beer-Sheva 84105, Israel.

*These authors contributed equally to this work
†Author for correspondence (abdu@bgu.ac.il)

Accepted 22 August 2011

both in the oocyte and in the bristle, Jvl protein accumulates in a region enriched with MT minus-ends. We discovered that expression of Jvl protein in the germline affects MT-dependent processes. Thus, our results identify the *jvl* gene as a novel microtubule-associated protein. Both loss- and gain-of-function analysis of this gene reveal that *jvl* regulates MT organization in the oocyte.

MATERIALS AND METHODS

Drosophila stocks

The following mutant and transgenic flies were used: grk^{HF} (Schüpbach, 1987; Neuman-Silberberg and Schüpbach, 1993); grk^{2B6}, grk^{2E12} (Neuman-Silberberg and Schüpbach, 1996); kinesin β-GAL insertion line KZ503 and the Nod-β GAL insertion line NZ143.2 (Clark et al., 1994; Clark et al., 1997); and Tau-GFP line 2.1 (Micklem et al., 1997). The $CG43162^{D590}$, jvl^{1}, Df(3R)Exel6172, Df(3R)Exel6275, w[1118]; CyO, P{Tub-PBac\T}2/wg[Sp-1] lines were all obtained from Bloomington Stock Center. Germline expression was performed with P{GAL4::VP16-nos.UTR}$CG6325^{MVD1}$ (which will be referred to as nos Gal4-VP16), P{GAL4-nos.NGT}40 (which will be referred to as nos-Gal4), P{matα4-GAL-VP16}V2H (which will be referred to as α-tub Gal4-2), P{matα4-GAL-VP16}V37 (which will be referred to as α-tub Gal4-3), which were obtained from Bloomington Stock Center. The UAS-RNAi for CG43162 was obtained from VDRC, Austria.

Cloning and transgenic flies

Initially, in our study we focused on a gene known as CG3563. However, in the 5.33 genome annotation release, CG3563 and CG33330 were merged to a new gene called CG43162. The CG43162 gene contains seven alternative splicing forms and in our study we used the CG43162-RA alternative splice form for cloning. For generating the pPGW-GFP:CG43612-RA construct, CG43612-RA was amplified from cDNA using primers designed for *Drosophila* gateway vectors. The PCR product was cloned into pDONOR vector using BP clonase (Invitrogen). The cloning into the final vectors (pPGW or pPFHW) was mediated by LR Clonase (Invitrogen).

To make the pUASp-CG43612-RA:GFP fusion construct, GFP was cloned into pUASp using *Kpn*I and *Xba*I restriction sites (called now pUASp-GFP). Then, *jvl* was cloned into pUASp-GFP using *Xba*I restriction sites. P-element-mediated germline transformation of these construct was carried out according to standard protocols (Spradling and Rubin, 1982).

Cloning of CG43162 into mammalian expression vector PL-452 N-EGFP was performed in two steps: the PCR product of CG43162 was cloned into pCR 4Blunt-TOPO donor vector (Invitrogen) and this construct was used for introduction of CG43162 into PL-452 N-EGFP using Gateway LR Clonase II kit (Invitogen).

Immunostaining and in situ hybridization

RNA in situ hybridization on ovaries and antibody staining of cells and ovaries was carried out as described previously (Abdu et al., 2006; Dubin-Bar et., 2008). For bristle immunostaining, tissues were treated as described by Bitan et al. (Bitan et al., 2010). The following primary antibodies were used: rabbit anti-Jvl (1:100), mouse anti-Spn-F (1:10, clone 8C10) (Abdu et al., 2006), mouse anti-Grk (1:10, clone 1D12) (Queenan et al., 1999), rabbit anti-Oskar (1:3000) (Vanzo and Ephrussi, 2002), mouse anti-α-tubulin (1:200, Sigma), mouse anti β-Gal (1:500, Promega), mouse anti-Orb 4H8 and 6H4 (1:10) (Lantz et al., 1992), rat anti HA (1:200, Roche Diagnostics) and rabbit anti Jvl (1:100). The secondary antibodies goat anti-mouse Cy2 and Cy3, and goat anti-rabbit Cy3 (Jackson ImmunoResearch) were used at a dilution of 1:100. The secondary antibody goat anti-rabbit Cy3 (Molecular Probes) was used at a dilution of 1:500. The following dyes were used: Oregon green 488 and Alexa Fluor 568 phalloidin (1:250, Molecular Probes), Hoechst (1:1000, Molecular Probes), wheat germ agglutinin (WGA) (20 μg, Molecular Probes). MT detection was carried out as described by Januschke et al. (Januschke et al., 2006). All pictures were imaged on Olympus FV1000 Laser-scanning confocal microscope.

Cell culture and transfections

$S2R^{+}$ and HEK293 cells were cultured and transfected as described by Dubin-Bar et al. (Dubin-Bar et al., 2008).

Generation of antibody for Jvl

An optimal antigen was designed and cloned as a fusion protein with a histidine tag. The protein was highly expressed in the pellet as inclusion bodies. Therefore, we purified the protein with Ni+ beads under denaturing conditions (8 M urea). After protein verification by MALDI-TOF mass spectrometry technique, we sent the purified protein to an external company (Hadar Biotech) for antibody production in rabbit.

Yeast two hybrid assay

Yeast two hybrid analysis was performed using the Yeast Two Hybrid Phagemid vector kit (Stratagene), following the manufacturer's instructions. The pAD-Spn-F plasmid was used as bait while plasmids encoding full-length Jvl protein and truncated versions were used as prey. The YRG2 host strain (Stratagene) was co-transformed with pAD-Spn-F and pBD-partner plasmids in all possible combinations using the LiAC method. Positive interactions were detected by selecting on SD-His plates.

GST pull-down assay

Spn-F protein was cloned into pGEX4 and $Jvl^{400-800}$ was cloned into pHIS-parallel1. Protein expression in Rosetta bacteria cells was induced by adding 1 mM IPTG overnight at 18°C. Glutathione-sepharose resin (a 10 μl bed volume) was added to 30 μg of GST-Spn-F or GST alone, and the mixture was incubated for 1 hour at 4°C. HIS-$Jvl^{400-800}$ was purified in accordance to manufacturer's instructions (Qiagen, The QIAexpressionist). GST-Spn-F or GST protein bound to glutathione-sepharose resin were incubated with purified HIS-$Jvl^{400-800}$ at 4°C overnight. The resin was then washed four times with 500 μl of PBS. The bound proteins were subjected to SDS-8% PAGE followed by western blotting using anti-HIS and anti-GST antibodies.

Scanning electron microscopy

Adult *Drosophila* were prepared and examined for scanning electron microscopy as described by Bitan et al. (Bitan et al., 2010).

RESULTS

Molecular characterization of *javelin-like* locus

Our previous results indicated that Spn-F and Ik2 form a complex that plays a role in MT organization during oogenesis and bristle development (Abdu et al., 2006; Dubin-Bar et al., 2008; Bitan et al., 2010). We decided to investigate their role in MT organization further by searching for new proteins that interact with Spn-F or Ik2. In a two-hybrid-based protein-interaction map of the fly proteome, several proteins were found to interact with Spn-F and Ik2 (Giot et al., 2003). Based on this protein list, a candidate RNAi screen was performed in our laboratory for the identification of novel *spn-F* and *ik2* interactors. As both *spn-F* and *ik2* mutants share similar bristle phenotypes (Abdu et al., 2006; Shapiro and Anderson, 2006; Bitan et al., 2010), we screened the candidate RNAi genes for bristle morphology defects. We screened 10 out of 15 new proteins that were found to interact with spn-F and with new ik2 interactor proteins, and found one novel candidate gene that showed bristle defects. Whereas in wild type, bristles taper along the bristle shaft into the bristle tip (Fig. 1A,A′), we found that RNAi-mediated downregulation of CG43162 in the bristle using neu-Gal4 driver resulted in a tapering bristle that ended with a swollen tip characterized by mis-oriented actin ridges (Fig. 1C) resembling the phenotype that was observed after RNAi-mediated downregulation of *spn-F* in bristles (Fig. 1B).

The CG43162 gene is located in position 88D2-D3 in the *Drosophila* genome. To find possible mutations in CG43162, we searched FlyBase for uncharacterized mutants that affect bristle

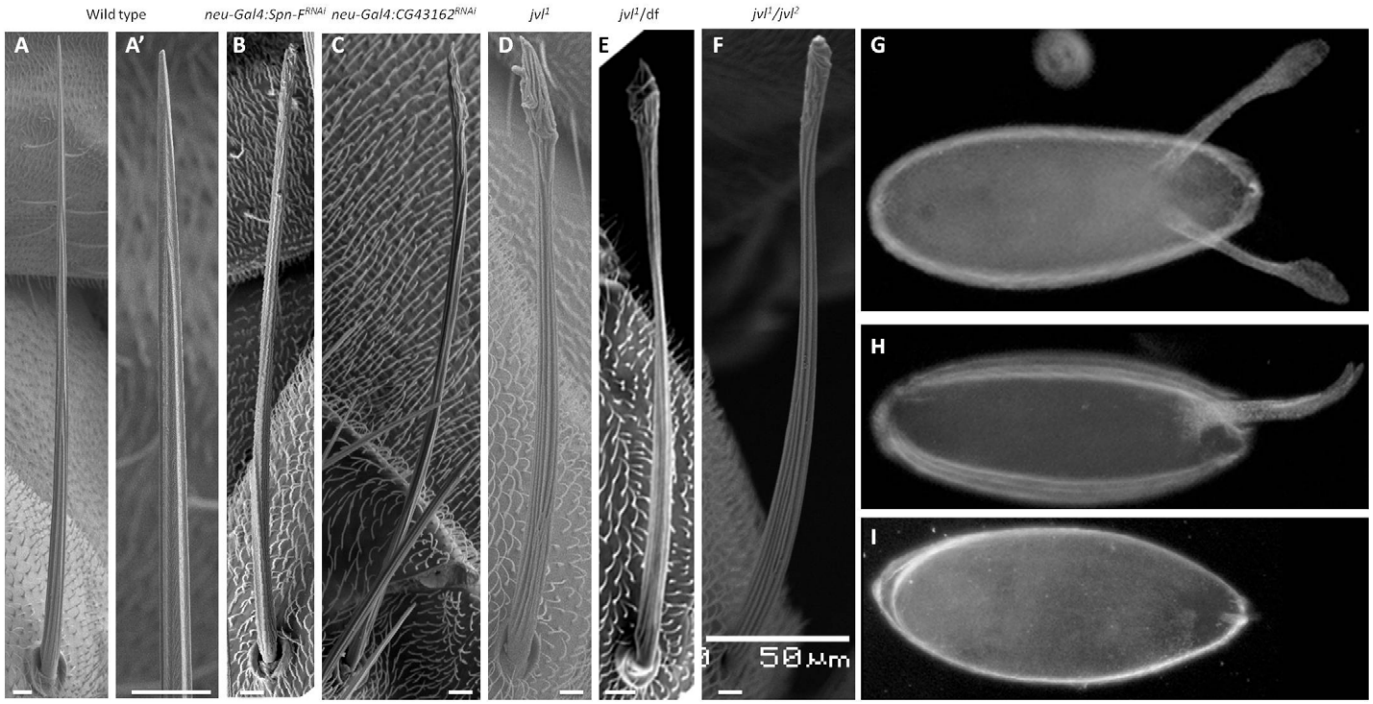

Fig. 1. Mutations in *jvl* affect bristle and egg chamber development. (**A**,**A′**) A wild-type bristle and an enlargement of the tip area. (**B**) Bristle from *neur-Gal4:UAS-spn-F*^{RNAi}. (**C**) Bristle from *neur-Gal4:UAS-CG43162*^{RNAi}. (**D**) *jvl*^{1} mutants bristle. (**E**) *jvl*^{1} hemizygous mutant bristle. (**F**) *jvl*^{1}/*jvl*^{2} mutant bristle. (**G-I**) Eggshells from *jvl* hemizygous females. (G) Wild type-like eggshell. (H) Ventralized eggshell with one appendage. (I) Strongly ventralized eggshell with no appendages. Scale bars: 5 μm.

morphology that were also mapped to this region. One such mutant is the *javelin-like* (*jvl*) gene. This mutation was identified in 1942 (FlyBase) and was mapped to region 88C2-88E3 (Nelson and Szauter, 1992); the gene affected by this mutation is still unknown. Mutations in *jvl* affect bristle tip morphology (Fig. 1D) in a similar way to RNAi-mediated downregulation of CG43162 (Fig. 1C), and are male and female fertile. Using deficiency mapping, we showed that *jvl* gene resides in region 88D5-D7, which includes 14 different genes, among them the CG43162 gene. There are nine known transposon insertions associated with CG43162 gene. Three of these lines are available, and only one of them, CG43162^{D590}, is homozygous lethal. Next, we examined whether these transposon-inserted flies in CG43162 failed to complement *jvl* mutant phenotype. We found that only the CG43162^{D590} line fails to complement the *jvl* bristle phenotype (Fig. 1F). Interestingly, both transheterozygous (*jvl*/CG43162^{D590}) and hemizygous females (*jvl*/*df*) were sterile and laid eggs with dorsal-ventral defects (Fig. 1H-I; Table 1). Therefore, we suggest that CG43162 and *jvl* correspond to the same gene locus and for the ease of reading we will refer to the spontaneous mutation in the original mutant stock of *jvl-jvl*^{1} and the CG43162^{D590} line as *jvl*^{2}.

In order to investigate the *jvl* gene further, we wanted to characterize the phenotypes of the two alleles *jvl*^{1} and *jvl*^{2}. *jvl*^{1} flies have bristle defects and the females are fertile, whereas *jvl*^{2} flies possess a lethal mutation, suggesting that *jvl*^{1} is a hypomorphic allele and *jvl*^{2} is a strong loss-of-function allele. We further characterized at what stage of development *jvl*^{2} mutant flies died. We found that *jvl*^{2} mutants die during embryonic development. However, *jvl*^{2} hemizygous flies die as pharate adults. These results indicate that the lethality in the embryonic stage in *jvl*^{2} homozygous flies is not due to CG43162 gene but is located in another region on the 3rd chromosome. Subsequently, we were able to use recombination to eliminate the lethality, which was indeed not associated with the mutation in the CG43162 gene.

In order to verify that CG43162 encodes *jvl*, we sequenced CG43162-coding region from genomic DNA of the jvl mutant stock and compared them with wild type. However, no mutations were found in the coding region of CG43162 gene in *jvl1* mutant. Next, we performed rescue experiments by expressing CG43162 protein in the background of *jvl* mutant. We created transgenic flies expressing CG43162 protein under the control of the UAS/Gal4 system. We tested the ability of CG43162 to rescue female sterility. To achieve this, we expressed the CG43162 protein in either *jvl*^{1} hemizygous or *jvl*^{1}/*jvl*^{2} ovary flies using *nos-Gal4*, which is specifically expressed in the germline in the ovary. We found that the expression of CG43162 protein in these mutants ovaries rescued female sterility. These results indicate that the CG43162 gene encodes the *jvl* gene.

Table 1. Relative percentages of the different eggshell phenotypes found in *jvl* transheterozygous and hemizygous females

Genotype	*n*	No appendages	Fused appendages	Wild type like
Wild type	465	0%	1%	99%
jv1^{1}/*CG43162*^{D590}	361	37%	40%	23%
jv1^{1}/Df	294	96%	2%	2%

jvl affects the dorsal-ventral polarity of the eggshell by affecting grk mRNA and protein localization

As mentioned above, jvl^1/jvl^2 and jvl^1 hemizygous mutants laid eggs with dorsal-ventral defects (Fig. 1, Table 1). As jvl^1 hemizygous females produced stronger phenotypes than jvl^1/jvl^2 (98% defective eggs compared with 77%, respectively) (Table 1), most of the analysis was performed on this genotype; thus, in the text we will refer to *jvl* mutant as to the hemizygous combination, unless noted otherwise. Defects in dorsal-ventral polarity can be due to mislocalization of *gurken* (*grk*) mRNA. In situ hybridization analysis with a *grk* probe was performed in *jvl* mutants and wild-type ovaries (Fig. 2). In wild-type ovaries *grk* mRNA localized to the future anterior-dorsal corner of the oocyte (Fig. 2A), whereas in *jvl* mutants ovaries, *grk* mRNA localized to the anterior cortex of the oocyte (Fig. 2B) or to ectopic sites in the middle of the oocyte (Fig. 2C). Next, we labeled wild-type and *jvl* mutant ovaries with antibodies for Grk protein. In wild-type ovaries during mid-oogenesis, Grk is restricted to the anterior-dorsal corner of the oocyte (Fig. 2E), whereas in *jvl* mutants, Grk protein localized in the oocyte in actin-enriched aggregates (Fig. 2H,I). In addition, during stage 8 of oogenesis, we observed some puncta of Grk protein in the follicle cells in *jvl* mutants (Fig. 2I). These results indicate that the dorsal-ventral defects of *jvl* mutant eggs are due to mislocalization of *grk* and impairment in the process that leads to determination of the dorsal fate of the egg and the embryo.

jvl also affects oskar and bicoid mRNA localization

Next we analyzed whether *jvl* also affects the localization of other maternal mRNAs, in particular the ones that determine the anterior-posterior axis of the embryo. In wild type during early stages of oogenesis (up to stage 7), *osk* mRNA fills the entire perinuclear space of the growing oocyte. By stage 8 *osk* mRNA is found throughout the oocyte but there is enrichment at the posterior pole and there is also an accumulation at the anterior end (Ephrussi et al., 1991). From stage 9 and later, *osk* mRNA is localized to the posterior end of the oocyte and initiates the development of the future germ cells and the abdomen of the embryo (Lehmann and Nüsslein-Volhard, 1986). During early stages and mid stages of oogenesis (up to stage 9), *osk* mRNA localization pattern in the oocyte of jvl^1 hemizygous females is similar to wild type (data not shown). Whereas in wild-type egg chambers at stage 9, *osk* mRNA and protein are localized to the posterior pole of the oocyte (Ephrussi et al., 1991) (Fig. 3A,C), in jvl^1 hemizygous egg chambers *osk* mRNA and protein are correctly localized but there is a reduction in *osk* levels compared with wild type. Moreover, in jvl hemizygous mutants, *osk* mRNA and protein are also found as large puncta close to the posterior (Fig. 3B,D).

Next, we studied the effect of *jvl* on the anterior organization of the oocyte. *bcd* mRNA normally localizes at the anterior of the oocyte from stage 8 and specifies anterior cell fate, including the head and thorax (Berleth et al., 1988). In wild-type stage 8 egg chambers, *bcd* mRNA indeed localized at the ends of the anterior margins of the oocyte (Fig. 3E, arrows); however, in jvl^1 hemizygous oocytes, *bcd* (Fig. 3F, asterisk) is no longer found at the anterior ring but it concentrated near the oocyte nucleus (Fig. 3F, arrow). Also at latter stages of egg chamber development in jvl^1 hemizygous oocytes, the level of *bcd* mRNA (Fig. 3H, asterisk) along the anterior margins of the oocyte is significantly reduced and it is particularly enriched close to the oocyte nucleus (Fig. 3H, arrow).

Actin and MT network in *jvl* mutants

As the correct localization of *grk*, *osk* and *bcd* mRNA within the oocyte rely on the cytoskeleton, we examined actin and MT organization in *jvl* mutant oocytes. We stained egg chambers with

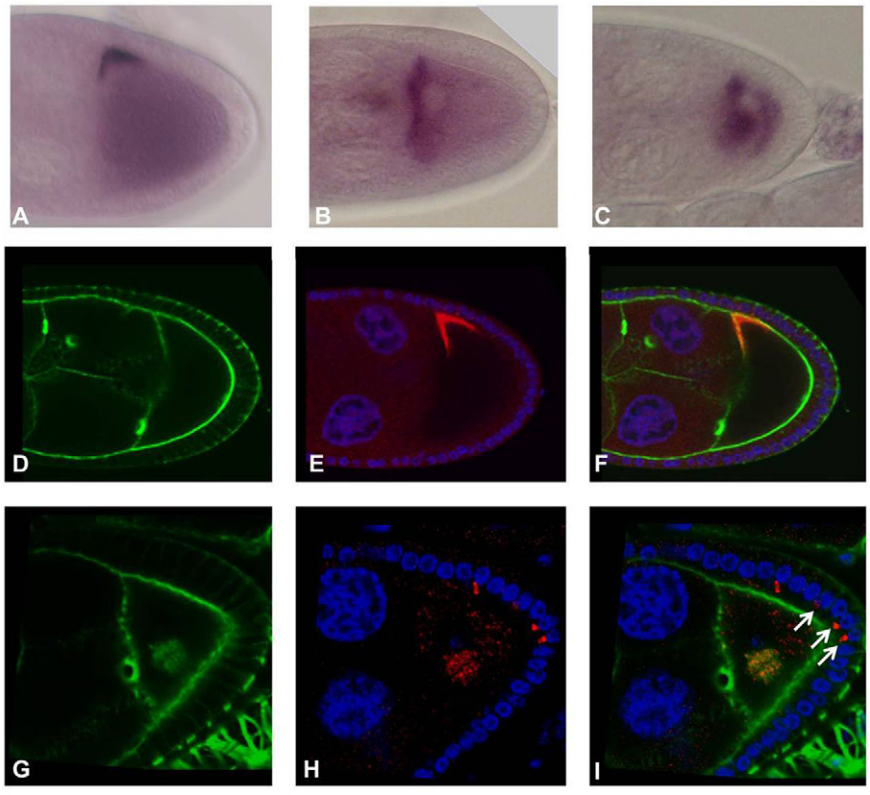

Fig. 2. *grk* mRNA and protein are mislocalized in *jvl* hemizygous egg chambers. (**A-C**) In situ hybridization analysis with *grk* mRNA probe. (A) Wild-type stage 9 egg chamber; (B,C) *jvl* hemizygous stage 9 egg chamber. (**D-I**) Confocal images of wild-type egg chamber (D-F) or a *jvl* hemizygous egg chamber (G-I) stained for actin in green (D,G), and for DNA in blue and for anti-Grk in red (E,H). (F,I) Merged pictures.

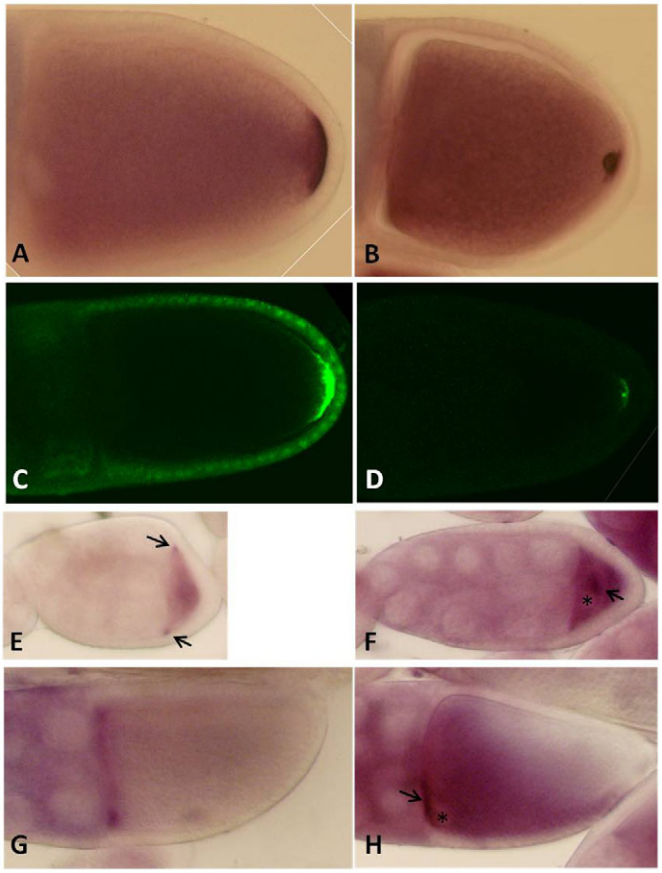

Fig. 3. *osk* mRNA and protein are mislocalized and *bcd* mRNA levels are reduced in *jvl* hemizygous egg chambers. (**A**,**B**) In situ hybridization analysis with *osk* mRNA probe in wild-type egg chamber (A) and *jvl* hemizygous egg chamber (B). (**C**,**D**) Confocal image of wild-type egg chamber (C) and *jvl* hemizygous egg chamber (D) stained with anti-Osk in green. (**E-H**) In situ hybridization analysis with *bcd* mRNA probe. (E) Wild-type stage 8 egg chamber, *bcd* mRNA (arrows). (F) *jvl* hemizygous stage 8 egg chamber, *bcd* (arrow), oocyte nucleus (asterisk). (G) Wild-type stage 10 egg chamber. (H) *jvl* hemizygous stage 10 egg chamber, *bcd* mRNA (arrow), oocyte nucleus (asterisk).

rhodamine-conjugated phalloidin and found that whereas in wild type, most actin was uniformly and evenly distributed at the cortical surface (Fig. 2D), in *jvl* mutants we observed ectopic sites of actin polymerization in the middle of the oocyte (Fig. 2G). Co-staining with Grk protein revealed that Grk protein colocalizes with the ectopic actin (Fig. 2I). For MT detection, we used Tau-GFP, which is a MT-binding protein (Mickelem et al., 1997), and anti α-tubulin**.** In wild-type stage 9 egg chambers, we found an enrichment of Tau-GFP at the anterior of the oocyte (Fig. 4A). However, in *jvl* mutants there is a reduction in Tau-GFP (Fig. 4B) levels in the anterior cortex and there is also an abnormal accumulation in discrete ‘dots’ around the oocyte nucleus (Fig. 4B′). Similar results were observed using anti α-tubulin antibodies (data not shown). As the organization of the MT network was impaired in *jvl*, we next studied its effect on MT polarity and functionality. In *jvl* mutants, as in wild-type egg chambers, the MT plus-end-directed motor kinesin was enriched at the posterior pole of the oocyte in a tight crescent (Fig. 4C,D). To analyze transport to the anterior pole, we used the MT minus-end marker, Nod:β-gal (Clark et al., 1997). In wild-type egg chambers at stages 8 to 10, Nod:KHC:β-gal is localized to the anterior margin of the oocyte and is enriched in the dorsoanterior corner adjacent to the oocyte nucleus (Fig. 4E). In jvl^{1} hemizygous mutants, Nod:KHC:β-gal could not be detected (Fig. 4F), suggesting that the MT minus-ends are not properly distributed along the anterior cortex during mid-oogenesis.

Jvl is associated with MT network

The CG43162 gene encodes for a protein with no homology outside of insects. Bioinformatics analysis revealed that the protein does not contain any known domain besides one coiled-coil domain. For further analysis of the *jvl* gene, we characterized Jvl protein localization. To achieve this, we first analyzed the localization of Jvl protein in $S2R^{+}$ cells and human cells. We cloned a GFP-tagged Jvl protein into a UAS vector and expressed it under the control of actin-Gal4 in Schneider cells. We found that this GFP fusion protein is localized to a filamentous structure that resembles the MT (Fig. 5B). Labeling of cells expressing GFP-Jvl with anti-α-tubulin (Fig. 5C) confirmed that CG43162 colocalizes with the MT network (Fig. 5D). Next, we decided to test the localization of Jvl in a heterologous system such as mammalian cells. To achieve this, we cloned CG43162 into a mammalian GFP-tagged expression vector, and expressed it in the human embryonic kidney cells (HEK239) cells. Jvl protein also colocalizes with the MT network in HEK239 cells, but seems to be more closely aligned with the MT network when compared with GFP-Jvl localization in Schneider cells (Fig. 5F). Moreover, expression of GFP-Jvl in both Schneider and HEK239 cells had no obvious effect on MT organization (Fig. 5, compare A with C and E with G).

To further analyze the function of *jvl* during oogenesis, we decided to generate an antibody for Jvl protein. Immunostaining with the antibody for Jvl protein demonstrated that in wild-type ovaries, the protein localizes to the posterior pole of the oocyte and around the nurse cell nuclei during early stages of oogenesis (Fig. 6A). During mid-oogenesis, the protein is localized all around the cortex with enrichment at the anterior pole (Fig. 6B). These results show that Jvl protein is enriched in regions where the MT minus-ends reside.

As mutations in *jvl* were primarily identified based on their effect on bristle morphology, we decided to test the localization pattern of this protein in the bristles. Using our antibody for Jvl protein, we found that the protein accumulates at the bristle tip (Fig. 6C,D and intensity profile of Jvl staining in Fig. 6G), where the MT minus-end marker Nod:KHC:β-gal, and Spn-F and Ik2 are enriched (Bitan et al., 2010). Next, we studied the localization pattern of Jvl protein in *jvl* mutants. As described above, genetics analysis showed that jvl^{2} is a strong loss-of-function allele, using anti-Jvl antibodies we were unable to detect Jvl protein in jvl^{2} bristles (Fig. 6E,F and intensity profile of Jvl staining in Fig. 6H), demonstrating the specificity of the antibody.

Next, we decided to study the localization pattern of GFP-Jvl during oogenesis. We generated transgenic flies expressing GFP-Jvl under the control of UAS/Gal4 system. We drove the expression of GFP-Jvl in the germline using *nos-Gal4* and found that in mid-oogenesis egg chambers GFP-Jvl is found at a perinuclear position in the nurse cells (Fig. 6D, arrow), and enriched at the membranes of the nurse cells and at the anterior end of the oocyte (Fig. 6D). Closer examination of the localization pattern in the nurse cell cytoplasm revealed that GFP-Jvl is found at filamentous structures that resemble the MT network (Fig. 6E,F). Indeed, staining with anti-α-tubulin antibodies (Fig. 6E) revealed that GFP-Jvl colocalizes with MTs (Fig. 6H). Thus, we believe that

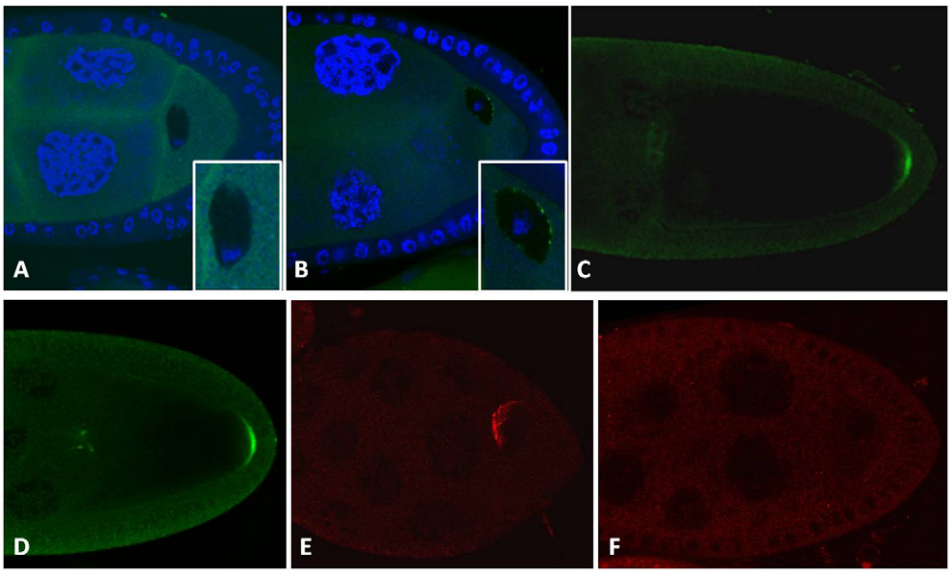

Fig. 4. *jvl* affects MT organization. (**A**,**B**) Expression of Tau-GFP in wild-type (A) and *jvl* hemizygous mutants (B). Tau-GFP is in green; DNA is in blue. Oocyte nucleus magnification (A,B, insets). (**C**,**D**) Localization of Kinesin-β-Gal in wild type (C) and *jvl* hemizygous mutants (D). (**E**,**F**) Localization of Nod-β-Gal in wild-type (E) and *jvl* hemizygous mutant (F) stage 8 egg chambers.

the sensitivity of GFP-Jvl, when compared with using anti-Jvl antibodies on fixed egg chambers, allows the detection of GFP-Jvl along the MT networks.

We also observed that *jvl* mRNA is localized asymmetrically in the oocyte and this localization is dependent on MT polarity within the oocyte (see Fig. S1 in the supplementary material).

Jvl changes the localization pattern of Spn-F protein

As mentioned above, a yeast two-hybrid study showed that Jvl interacts with Spn-F. In light of this finding, we decided to examine the localization pattern of these proteins in S2R$^+$ and in the ovary. Expression of mCherry-tagged Spn-F in S2R$^+$ cells revealed that the protein is found in cytoplasmic punctate structures (Dubin-Bar et al., 2008) (Fig. 7B). Here, we showed that GFP-Jvl is localized to the MT network in S2R$^+$ (Fig. 5A; Fig. 7A). Interestingly, when mCherry Spn-F was co-expressed with GFP-Jvl, we found that Spn-F now colocalized with Jvl to the MT network (Fig. 7E), which suggests that Jvl affects Spn-F localization. We also found that GFP-Jvl also changes the localization pattern of Ik2 as it does for Spn-F (data not shown).

Next, we studied the ovarian localization pattern of Spn-F in transgenic flies expressing GFP-Jvl. In wild-type egg chambers during mid-oogenesis, Spn-F localized along the anterior margins of

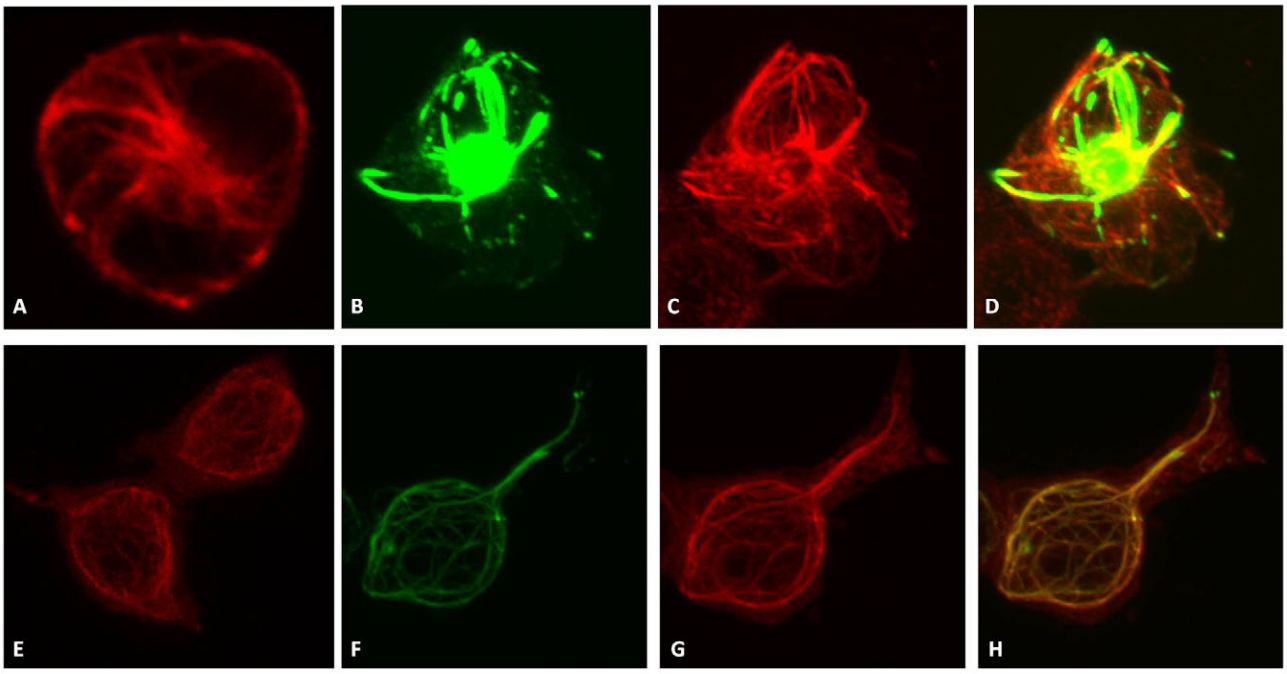

Fig. 5 Jvl colocalizes with the MT in Schneider cells and HEK293 cells. (**A-H**) Confocal projections of Schneider (A-D) and HEK293 (E-H) cells, expressing GFP-Jvl (B,F green) and stained with antibody for α-tubulin (C,G red). (A,E) Schneider (A) and HEK293 (E) cells stained with antibody for α-tubulin (red). (D,H) Merged pictures.

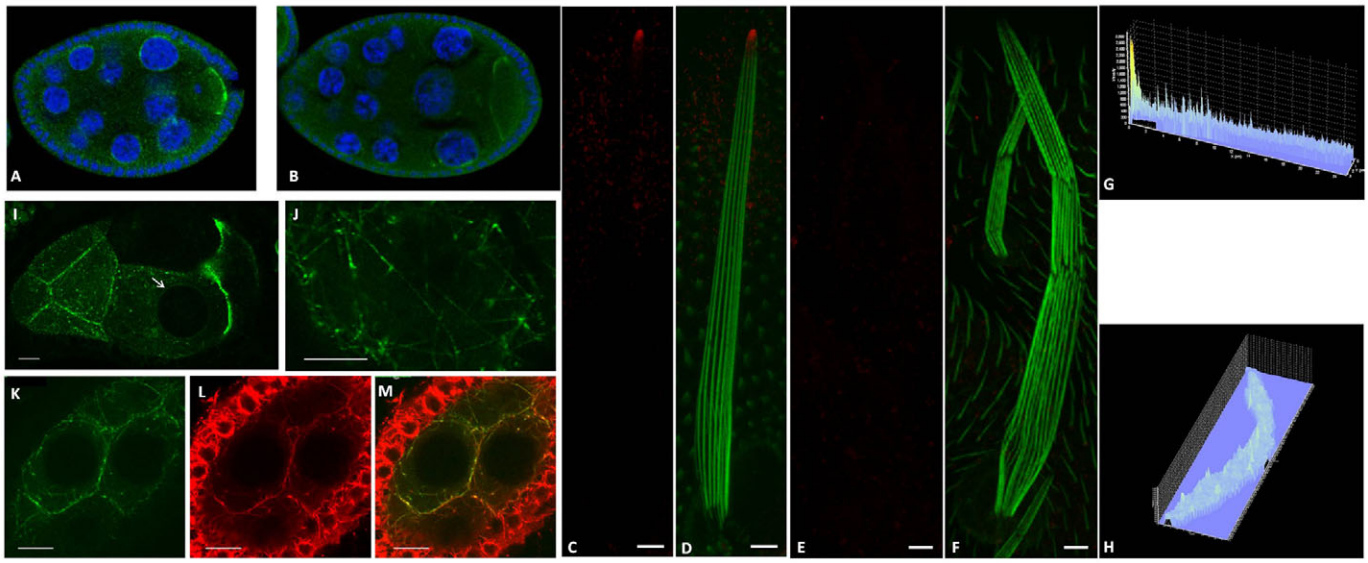

Fig. 6. Jvl protein is localized to MT minus-end enriched regions. (**A**,**B**) Confocal images of different stages of wild-type egg chambers stained to detect anti-Jvl (green) or DNA (blue) (A,B). (A) Stage 5 egg chamber; (B) stage 8 egg chamber. (**C-H**) Confocal projections of a wild-type (C,D) or *jvl*^{2} mutant bristles (E,F) stained with anti-Jvl (green) and with Alexa Fluor phalloidin (red). Jvl is enriched at the bristle tip in wild type (C,D; intensity profile in G) but is missing from the bristle shaft in *jvl*^{2} mutants (E,F; intensity profile in H). (**I-M**) Confocal images of egg chambers from GFP-Jvl::*nos-Gal4* flies expressing GFP-Jvl (green) and stained with anti α-tubulin antibody to visualize tubulin (red) (L). Scale bars: 10 μm.

the oocyte and in punctated form in the nurse cells (Abdu et al., 2006) (Fig. 7F). In GFP-Jvl-expressing egg chambers Spn-F is colocalized with GFP-Jvl along the anterior margins of the oocyte and to the nurse-cells membranes (Fig. 7I). Closer examination showed that Spn-F is also colocalized with GFP-Jvl to filamentous-like structures (Fig. 7L). As was shown in Fig. 6 (Fig. 7K-M), these structures localized with MT. These results support our results in the in S2R^{+} cells, which showed that Jvl affects Spn-F protein localization.

Jvl interacts physically with Spn-F

To understand better the nature of interaction between Jvl and Spn-F, we performed yeast two hybrid assay and GST pull-down analysis. First, we mapped the region in Jvl protein that is sufficient for interaction with Spn-F. To achieve this, we created several truncated versions of Jvl and tested their ability to interact with Spn-F using yeast two hybrid analysis. We found that full-length Jvl, as well as the Jvl$^{1\text{-}800}$ truncation, interact with Spn-F (Fig. 8B). However, the Jvl$^{1\text{-}600}$ truncated form failed to interact with Spn-F (Fig. 8B). Next, we analyzed the interaction between Spn-F and a truncated version of Jvl that extends from 400 amino acids to 800 amino acids (Jvl$^{400\text{-}800}$), and found that this part was sufficient to interact with Spn-F (Fig. 8B). To prove further that this truncated version is sufficient for direct interaction with Spn-F, we performed a GST pull-down assay. We found that Jvl$^{400\text{-}800}$ mediates direct interaction with Spn-F (Fig. 8C). Interestingly, Jvl$^{400\text{-}800}$ contains one coiled-coil domain that extends from 705 amino acids to 749 amino acids (Fig. 8A), which might mediate the interaction between Spn-F and Jvl.

Overexpression of Jvl in the germline affects oocyte growth, localization and oocyte nucleus anchoring

In order to study the effect of overexpression of Jvl protein in the ovary, we generated a transgenic line under the control of UAS-Gal4. To express Jvl at low levels, we used the *nos-Gal4* and α*tubGal4-2* driver lines. For moderate expression, we used the *nosGal 4-VP16* driver and for high expression levels we used the α*tubGal4-3* driver (Januschke et al., 2002). The difference in the expression between α*tubGal4-2* and α*tubGal4-3* is probably due to the fact that they are located on different chromosomes. Low expression levels of Jvl had no effect on the ovarian phenotype. However, high expression caused small (98%, *n*=34) and mislocalized (97%, *n*=34) oocytes (Fig. 9B). Moreover, moderate expression led to mislocalization of the oocyte nucleus in stage 9 egg chambers (15%, *n*=30) (Fig. 9D).

As mentioned above, expression of Jvl with α*tubGal4-3* caused smaller and mislocalized oocytes. We noticed that overexpression of Jvl in the ovaries had no effect on egg chamber size, but did affect oocyte growth at stages 6 to 8, suggesting that transport from the nurse cells to the oocyte was impaired. If, indeed, this process is defective, we expect to see an effect on transport of determinants from the nurse cells to the oocyte. Therefore, we decided to stain Jvl/αtubGal4 3 ovaries with an antibody for oo18 RNA binding (orb), an RNA-binding protein (Lantz et al., 1992). In wild type, during early stages of oogenesis, *orb* mRNA is transported from the nurse cells to the oocyte in a microtubule-dependent manner (Pokrywka and Stephenson, 1995; Lantz et al., 1992). Later, in vitellogenic egg chambers, high levels of Orb protein accumulate in the cortical cytoplasm around the entire circumference of the oocyte (Fig. 9A). However, in the egg chambers of flies overexpressing Jvl, Orb protein was seen in the nurse cells, but failed to accumulate in the small oocyte (Fig. 9B). These results support the hypothesis that the MT-dependent transport from the nurse cells to the oocyte was damaged by overexpression of Jvl.

Another effect of overexpression of Jvl under the control of α*tubGal4-3* is related to the localization pattern of the oocyte within the egg chamber. In wild-type egg chambers, the oocyte is localized to the most posterior position (Fig. 9A). However, in Jvl overexpressing egg chambers, the oocyte is no longer found at the most posterior position (97%, *n*=34, Fig. 9B).

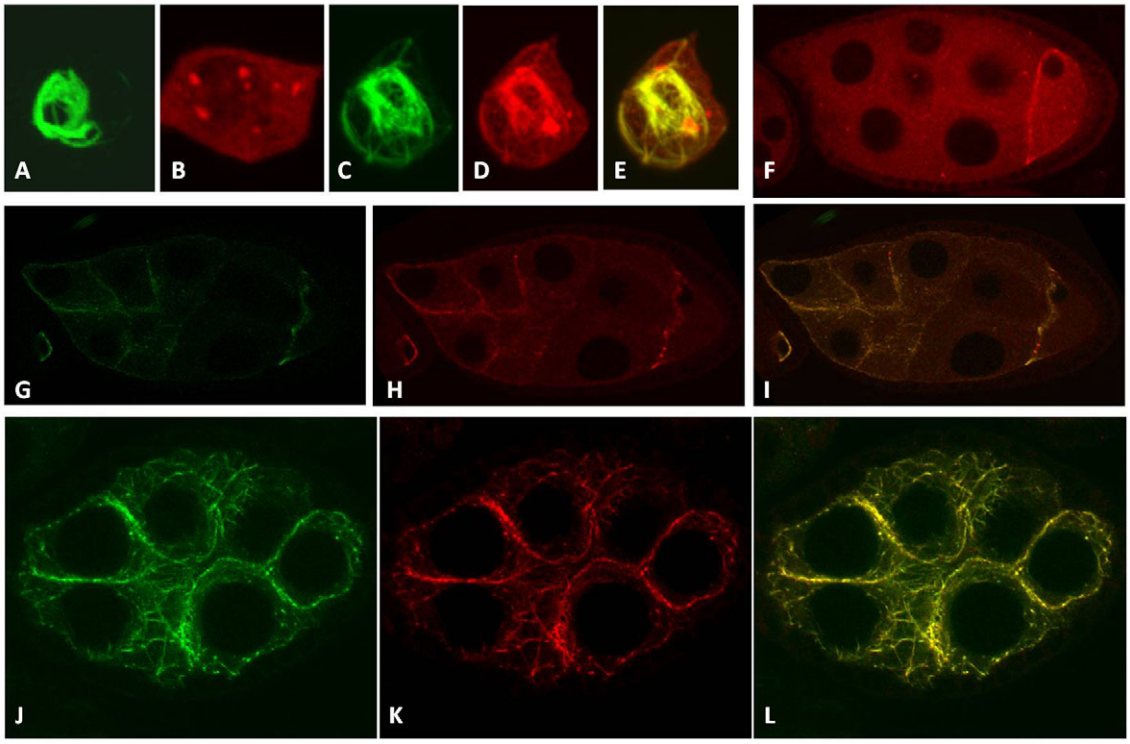

Fig. 7. Jvl changes Spn-F protein localization. (**A-E**) Confocal projections of: (A) S2R$^+$ expressing GFP-Jvl; (B) S2R$^+$ expressing mCherry-Spn-F; (C,D) S2R$^+$ co-expressing GFP-Jvl (C) and mCherry-Spn-F (D). (E) Merged picture. (**F-L**) Confocal images of stage 9 egg chambers stained for anti-Spn-F (red) from: (F) wild-type and (G-L) transgenic flies expressing GFP-Jvl (G,J) and stained to detect Spn-F protein. (I,L) Merged pictures.

As described above, expression of Jvl under the control of nos Gal4-VP16 led to oocyte nucleus mislocalization. Whereas in wild type, the oocyte nucleus is localized at the dorsal-anterior corner of the oocyte, where it is tightly attached to both the lateral and anterior cortices (Fig. 9C), we noticed that in 15% (n=30) of Jvl/nos Gal4-VP16 stage 9 oocytes, the nucleus was mislocalized (Fig. 9D) and found in the middle of the oocyte, close to the lateral cortex (Fig. 9D). In order to examine anchoring of the nucleus to the anterior cortex of the oocyte, optical cross- and vertical sections were taken using a confocal microscope. Analysis of these sections show that the nucleus attached only to the lateral cortex (Fig. 9D) and not to both the lateral and anterior cortices, as it did in the wild type (Fig. 9C).

DISCUSSION

CG43162 encodes the *javelin-like* gene

In order to investigate further the role of Spn-F in MT organization, we decided to search for new proteins that interact with Spn-F or Ik2. This study led to identification of the gene CG43162 as a novel MT-associated protein, which is part of this complex. Moreover, our study showed that CG43162 encodes the *javelin-like* (*jvl*) gene. Several lines of evidence suggest that that *jvl* encodes the CG43162 gene: (1) Using fine deficiency mapping of *jvl* mutants showed that *jvl* is found in CG43162 region; (2) we showed that downregulation of CG43162 specifically in the bristles led to defects in bristle morphology,

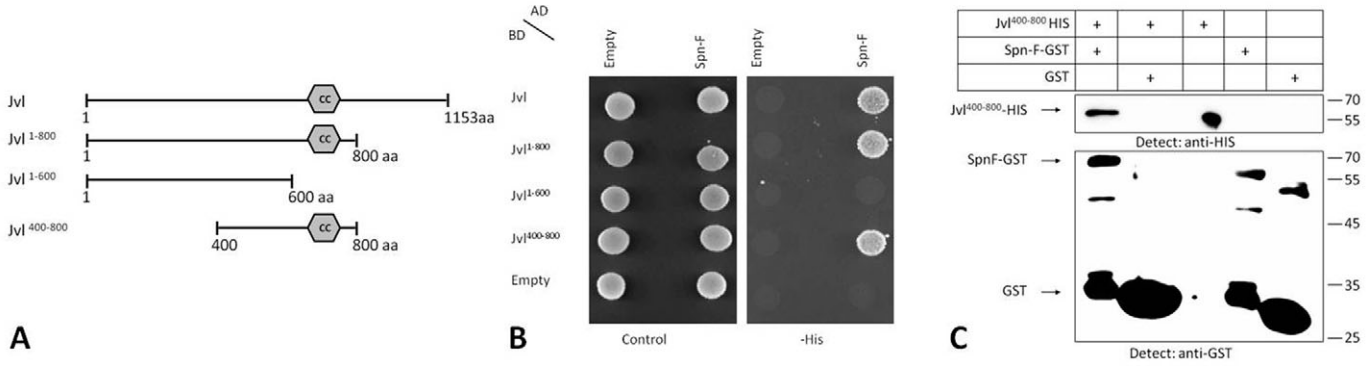

Fig. 8. Jvl interacts physically with Spn-F. (**A**) Schematic diagram of full Jvl protein and truncated proteins used in B and C. Bioinformatics analysis revealed that the protein contains one coiled-coil domain extending from amino acid 705 to amino acid 749 (hexagon). (**B**) Mapping of the binding domain of Jvl to Spn-F by yeast two hybrid assay. (**C**) GST pull-down with full-length recombinant GST-Spn-F and HIS-Jvl$^{400-800}$. The beads fraction was analyzed by western blotting with anti-HIS and anti-GST antibodies.

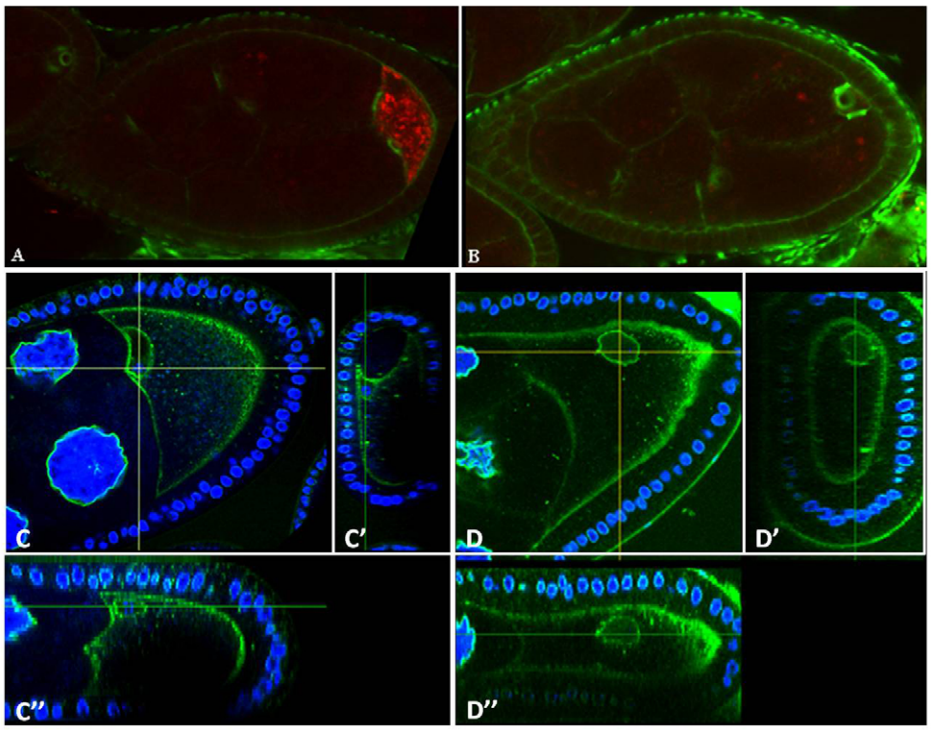

Fig. 9. Overexpression of Jvl affects MT-dependent processes during oogenesis. (**A**,**B**) Confocal images of wild-type (A) and GFP-Jvl::*αtubGal4-3* (B) stage 8 egg chambers stained with phalloidin (green) and anti-Orb (red). (**C-D″**) Confocal projections of egg chambers stained for DNA (blue) and nuclear membranes (WGA-green). The yellow lines indicate the planes for the optical cross-sections (C′,D′) and the vertical sections (C″,D″). (C-C″) Wild-type stage 9 egg chamber. (D-D″) GFP-Jvl::*nosGal 4-VP16* stage 9 egg chamber.

similar to the defects found in *jvl* mutants; 3) furthermore, a mutation in CG43162 ($CG43162^{D590}$) failed to complement *jvl* in both ovarian and bristle phenotypes, suggesting that $CG43162^{D590}$ and *jv*l are two different alleles of the same gene; and (4) we found that expression of CG43162 protein in oocytes rescued *jvl* female sterility. Considering all of these results, we conclude that the CG43162 gene encodes *jvl*.

Moreover, we suggest that Jvl is part of the Spn-F and Ik2 complex, based on the following evidence: (1) Spn-F physically interacts with Jvl (this study, yeast two hybrid and GST pull-down assays); (2) Spn-F physically interacts with Ik2 (Dubin-Bar et al., 2008); (3) *jvl* shares similar mRNA localization and bristle defects to *spn-F* and *ik2*; (4) Spn-F and Ik2 colocalize with Jvl to MT, where Jvl determines this localization pattern.

Jvl is an MT-associated protein

For further analysis of the *jvl* gene, we characterized Jvl protein localization. For this purpose, we first analyzed the localization of Jvl protein in $S2R^{+}$ cells and human cells. We showed that GFP-Jvl fusion protein was localized to the MT network. Next, we analyzed the localization pattern of Jvl during oogenesis. Using an antibody raised against the Jvl protein, we found that Jvl is localized to the region where the MT minus-ends reside. At early stages of oogenesis, Jvl protein localizes as a tight crescent in the posterior pole of the oocytes. During mid-oogenesis, Jvl protein is localized all around the cortex, with enrichment at the anterior pole. We also demonstrated that GFP-Jvl colocalizes with MTs in the nurse cells. Moreover, in the bristles, GFP-Jvl is localized asymmetrically, accumulating at the bristle tip, where other MT minus-end markers are found. Considering our results, indicating that Jvl localizes with the MT network in $S2R^{+}$ and human cells along with its localization in the egg chamber and developing bristle, we conclude that Jvl protein is associated with the MT network, specifically with the MT minus-ends.

jvl mutant affects MT organization in the oocyte

We demonstrated that jvl^{1} mutants are female fertile. However, flies hemizygous for jvl^{1} and flies transheterozygous for *jvl* (jvl^{1}/jvl^{2}) are female sterile. Beside sterility, we noticed that the *jvl* mutant females laid eggs with dorsal-ventral defects. Determination of dorsal-ventral polarity of the eggshell depends on Grk protein signaling (Neuman-Silberberg and Schupbach, 1993; Neuman-Silberberg and Schupbach, 1996). We showed that, in the hemizygous mutants, *grk* mRNA localizes in the anterior margins of the oocyte and in ectopic sites inside the oocyte. It has been suggested that *grk* mRNA moves in two distinct steps, both of which require MT and the motor protein *Dynein* (MacDougall et al., 2003). Each step depends on a different MT network. First *grk* mRNA moves towards the anterior of the oocyte, where it localizes transiently, and then to its final localization in the dorsal anterior corner of the oocyte. In *jvl* mutants, *grk* mRNA does not reach its final localization in the dorsal anterior corner of the oocyte, suggesting that the MT network upon which this step depends might be impaired in *jvl* mutants. This MT network is specifically associated with the oocyte nucleus and the minus-end in the dorsal-anterior corner of the oocyte (MacDougall et al., 2003). Next, we found that Grk protein in *jvl* mutants is also mislocalized. We show that Grk protein is colocalized with ectopic actin puncta close to the anterior of the oocyte. This localization pattern is also observed in *Bicaudal-C* and *trailer-hitch* mutants (Wilhelm et al., 2005; Snee and Macdonald, 2009). It has been suggested that the sequestration of Grk in the actin cages interfered with the signaling to the follicle cells (Snee and Macdonald, 2009); therefore, we suggest that sequestration of Grk in the actin cages in *jvl* mutant females similarly led to the dorsal-ventral polarity defects of the eggshell. In addition to the effect on *grk* mRNA and protein localization, *jvl* also affects *bcd* and *osk* mRNA localization. In wild-type, *bcd* mRNA is localized to the anterior pole of the oocyte facing the nurse cells, whereas *osk* mRNA is localized to the opposite posterior pole. The polar localization of these two mRNAs is

maintained throughout the rest of oogenesis and well into early embryogenesis (St Johnston and Nusslein-Volhard, 1992). The anterior localization of *bcd* requires both intact MTs and dynein motor protein function (Weil et al., 2006; Weil et al., 2008). *osk* localization to the posterior pole is achieved by two phases of transport: long-range MT-dependent transport by kinesin to the posterior, followed by actomyosin V-dependent positioning at the oocyte cortex (Krauss et al., 2009; Zimyanin et al., 2008).

What could be the function of Jvl protein during oogenesis? The effects of *jvl* on *grk* and *bcd* mRNA localization, along with the particular changes affecting cytoskeletal organization close to the oocyte nuclear membrane as evident for Nod:KHC:β-gal localization and Tau mislocalization, suggest that *jvl* might be involved in either transport to the minus-end of MTs or in the organization of the minus-ends of the microtubule around the oocyte nucleus, as been suggested for its interactor, Spn-F (Abdu et al., 2006). However, we also noticed that in *jvl* mutants, *osk* mRNA and protein are mislocalized. These phenotypes are probably not due to defects in either transport or organization of the MT plus-end, as the plus-end motor protein Kinesin I was properly localized as in the wild type. Examination of the cytoskeleton components of the oocyte shows that both actin and MTs are misorganized in *jvl* mutants. The MT levels along the anterior cortex of the oocyte were reduced with specific effects on the MT that surrounds the oocyte nucleus. However, ectopic aggregations of the actin cages were found in the middle of the oocyte. The defects in the organization of both actin and MT network, together with the defects in *osk* mRNA and protein localization, suggest that *jvl* could provide a connection between the actin and MT network. In summary, our results suggest that *jvl* plays a role in organization of the MT in the oocyte or in the stabilization of the connection between MT and actin cytoskeleton in the oocyte.

Overexpression of Jvl affects oocyte growth and oocyte nucleus localization

In this study, we also examined the effects of overexpression of Jvl in the germline. We have shown that overexpression of Jvl with different germline-specific Gal 4 affects oocyte growth, oocyte localization and, in later stages, oocyte nucleus localization. Interestingly enough, all of these phenotypes could arise from effects on MT network function.

Oocyte growth depends on several processes: early in oogenesis, until stage 7, the oocyte grows at approximately the same rate as a single nurse cell. At these stages, oocyte growth is due to the transport of mRNAs and proteins, including products of early pattern-formation genes from the nurse cells to the oocyte. This transport is a microtubule-dependent process (Koch and Spitzer, 1983). Later in oogenesis, after stage 7, oocyte growth depends on the transport of components such as lipid droplets, mitochondria and other single particles from the nurse cells into the oocyte. This transport is an actin-dependent process (Bohrman and Biber, 1994). Beginning in stage 8, the oocyte expands through the uptake of yolk from the surrounding follicle cells and hemolymph. Consequently, oocyte growth is more rapid than nurse cell growth (Swan and Suter, 1996). During stage 11, the remaining nurse cell cytoplasm is rapidly transferred to the oocyte, resulting in doubling the oocyte volume (Theurkauf, 1994). Overexpression of Jvl affects oocyte growth during stage 6 to stage 8, although the egg chamber size seems to be similar to that of wild-type stage 6 to 8 egg chambers. In these stages, oocyte growth depends on the transport of nutrients from the nurse cells to the oocyte, suggesting that overexpression of Jvl disrupted this transport. The fact that Orb protein is not detected in Jvl-overexpressing small oocytes strengthens this possibility.

Another phenotype that was obtained in moderate overexpression of Jvl is mislocalization of the oocyte nucleus in 15% of stage 9 egg chambers. During early stages of oogenesis, the oocyte nucleus localizes to the posterior pole of the oocyte. After stage 7, following Grk signal and reorganization of the MT network, the nucleus migrates towards the anterodorsal corner of the oocyte (González-Reyes et al., 1995; Roth et al., 1995). Positioning of the oocyte nucleus involves two anchoring steps: first anchoring to the lateral membrane, which requires dynein but not kinesin motor protein; and, second, after it localizes to the anterodorsal corner, anchoring to the anterior cortex of the oocyte, which requires both dynein and kinesin motor proteins (Duncan and Warrior, 2002; Januschke et al., 2002). Moreover, nucleus anchoring also requires correct organization of the MT scaffold that surrounds the oocyte nucleus (Januschke et al., 2002). Moderate expression of Jvl did not affect nucleus position in stage 8 egg chambers. At this stage, the nucleus was always at the dorsal anterior corner, as in the wild type. This finding implies that anchoring to the lateral cortex and migration of the oocyte nucleus is not affected in Jvl-overexpressing ovaries. However, the anchoring of the nucleus to the anterior membrane was affected. This could be due to misorganization of the MT scaffold that surrounds the nucleus. Thus, our results demonstrate that overexpression of Jvl protein affects MT-dependent processes such as transport of determinants from the nurse cells to the oocyte, and anchoring of oocyte nucleus to the anterior cortex of the oocyte. Taking into account the phenotypes detected in *jvl* mutants, our finding that Jvl is an MT-associated protein, together with the effects of Jvl overexpression on MT-dependent processes during oogenesis, it seems likely that *jvl* has a role in MT organization during oogenesis.

Most importantly, although *jvl* encodes for a protein with no homology beside insects, its association with MT network in mammalian cells, along with its effect on MT network in *Drosophila*, may suggest the existence of mammalian protein(s) with a function analogous to Jvl.

Acknowledgements

We thank Trudi Schüpbach, Shari Carmon, Ben-Zion Shilo, VDRC Austria and the Bloomington stock center for generously providing fly strains and reagents. We also thank Trudi Schüpbach for comments on the manuscript.

Funding

This research was supported by Israel Science Foundation [968/10 to U.A.].

Competing interests statement

The authors declare no competing financial interests.

Supplementary material

Supplementary material for this article is available at
http://dev.biologists.org/lookup/suppl/doi:10.1242/dev.069161/-/DC1

References

Abdu, U., Bar, D. and Schüpbach, T. (2006). *spn-F* encodes a novel protein that affects oocyte patterning and bristle morphology in *Drosophila*. *Development* **133**, 1477-1484.

Berleth, T., Burri, M., Thoma, G., Bopp, D., Richstein, S., Frigerio, G., Noll, M. and Nüsslein-Volhard, C. (1988). The role of localization of bicoid RNA in organizing the anterior pattern of the *Drosophila* embryo. *EMBO J.* **7**, 1749-1756.

Bettencourt-Dias, M., Giet, R., Sinka, R., Mazumdar, A., Lock, W. G., Balloux, F., Zafiropoulos, P. J., Yamaguchi, S., Winter, S., Carthew, R. W. et al. (2004). Genome-wide survey of protein kinases required for cell cycle progression. *Nature* **432**, 980-987.

Bitan, A., Guild, G. M., Bar-Dubin, D. and Abdu, U. (2010). Asymmetric microtubule function is an essential requirement for polarized organization of the *Drosophila* bristle. *Mol. Cell. Biol.* **30**, 496-507.
Bohrmann, J. and Biber, K. (1994). Cytoskeleton-dependent transport of cytoplasmic particles in previtellogenic to mid-vitellogenic ovarian follicles of *Drosophila*: time-lapse analysis using video-enhanced contrast microscopy. *J. Cell Sci.* **107**, 849-858.
Clark, I., Giniger, E., Ruohola-Baker, H., Jan, L. Y. and Jan, Y. N. (1994). Transient posterior localization of a kinesin fusion protein reflects anteroposterior polarity of the *Drosophila* oocyte. *Curr. Biol.* **4**, 289-300.
Clark, I. E., Jan, L. Y. and Jan, Y. N. (1997). Reciprocal localization of Nod and kinesin fusion proteins indicates microtubule polarity in the *Drosophila* oocyte, epithelium, neuron and muscle. *Development* **124**, 461-470.
Driever, W. and Nusslein-Volhard, C. (1988a). A gradient of bicoid protein in *Drosophila* embryos. *Cell* **54**, 83-93.
Driever, W. and Nusslein-Volhard, C. (1988b). The bicoid protein determines position in the *Drosophila* embryo in a concentration-dependent manner. *Cell* **54**, 95-104.
Dubin-Bar, D., Bitan, A.,Bakhrat, A., Kaiden-Hasson, R., Etzion, S., Shaanan, S. and Abdu, U. (2008). The *Drosophila* IKK-related kinase (Ik2) and Spindle-F proteins are part of a complex that regulates cytoskeleton organization during oogenesis. *BMC Cell Biol.* **9**, 51.
Duncan, J. E. and Warrior, R. (2002). The cytoplasmic dynein and kinesin motors have interdependent roles in patterning the *Drosophila* oocyte. *Curr. Biol.* **12**, 1982-1991.
Ephrussi, A., Dickinson, L. K. and Lehmann, R. (1991). *oskar* organizes the germ plasm and directs localization of the posterior determinant *nanos*. *Cell* **66**, 37-50.
Giot, L., Bader, J. S., Brouwer, C., Chaudhuri, A., Kuang, B., Li, Y., Hao, Y. L., Ooi, C. E., Godwin, B., Vitols, E. et al. (2003). A protein interaction map of *Drosophila melanogaster*. *Science* **302**, 1727-1736.
González-Reyes, A., Elliott, H. and St Johnston, D. (1995). Polarization of both major body axes in *Drosophila* by gurken-torpedo signalling. *Nature* **375**, 654-658.
Januschke, J., Gervais, L., Dass, S., Kaltschmidt, J. A., Lopez-Schier, H., St Johnston, D., Brand, A. H., Roth, S. and Guichet, A. (2002). Polar transport in the *Drosophila* oocyte requires Dynein and Kinesin I cooperation. *Curr. Biol.* **12**, 1971-1981.
Januschke, J., Gervais, L., Gillet, L., Keryer, G., Bornens, M. and Guichet, A. (2006). The centrosome- nucleus complex and microtubule organization in the *Drosophila* oocyte. *Development* **133**, 129-139.
Koch, E. A. and Spitzer, R. H. (1983). Multiple effects of colchicine on oogenesis in *Drosophila*: induced sterility and switch of potential oocyte to nurse-cell developmental pathway. *Cell Tissue Res.* **228**, 21-32.
Krauss, J., López de Quinto, S., Nüsslein-Volhard, C. and Ephrussi, A. (2009). Myosin V regulates oskar mRNA localization in the *Drosophila* oocyte. *Curr. Biol.* **19**, 1058-1063.
Kuranaga, E., Kanuka, H., Tonoki, A., Takemoto, K., Tomioka, T., Kobayashi, M., Hayashi. S. and Miura, M. (2006). Drosophila IKK-related kinase regulates nonapoptotic function of caspases via degradation of IAPs. *Cell* **126**, 583-596.
Lantz, V., Ambrosio, L. and Schedl, P. (1992). The *Drosophila* orb gene is predicted to encode sex-specific germline RNA-binding proteins and has localized transcripts in ovaries and early embryos. *Development* **115**, 75-80.
Lee, H. H., Jan, L. Y. and Jan, Y. N. (2009). *Drosophila* IKK-related kinase Ik2 and Katanin p60-like 1 regulate dendrite pruning of sensory neuron during metamorphosis. *Proc. Natl. Acad. Sci. USA* **106**, 6363-6368.
Lehmann, R. and Nüsslein-Volhard, C. (1986). Abdominal segmentation, pole cell formation, and embryonic polarity require the localized activity of oskar, a maternal gene in *Drosophila*. *Cell* **47**, 141-152.
MacDougall, N., Clark, A., MacDougall, E. and Davis, I. (2003). *Drosophila gurken* (TGFα) mRNA localizes as particles that move within the oocytein two dynein-dependent steps. *Dev. Cell* **4**, 307-319**.**
Micklem, D. R, Dasgupta, R., Elliott, H., Gergely, F., Davidson, C., Brand, A., González-Reyes, A. and St Johnston, D. (1997). The mago nashi gene is required for the polarization of the oocyte and the formation of perpendicular axes in *Drosophila*. *Curr. Biol.* **7**, 468-478.
Nelson, C. R. and Szauter, P. (1992). Cytogenetic analysis of chromosome region 89A of *Drosophila melanogaster*: isolation of deficiencies and mapping of Po, Aldox-1 and transposon insertions. *Mol. Gen. Genet.* **235**, 11-21.
Neuman-Silberberg, F. S. and Schüpbach, T. (1993). The *Drosophila* dorsoventral patterning gene *gurken* produces a dorsally localized RNA and encodes a TGF-α-like protein. *Cell* **75**, 165-174.
Neuman-Silberberg, F. S. and Schüpbach, T. (1996). The *Drosophila* TGF alpha-like protein Gurken: expression and cellular localization during *Drosophila* oogenesis. *Mech. Dev.* **59**, 105-113.
Oshima, K., Takeda, M., Kuranaga, E., Ueda, R., Aigaki, T., Miura, M. and Hayashi, S. (2006). IKK epsilon regulates F actin assembly and interacts with *Drosophila* IAP1 in cellular morphogenesis. *Curr. Biol.* **16**, 1531-1537.
Otani, T., Oshima, K., Onishi, S., Takeda, M., Shinmyozu, K., Yonemura, S. and Hayashi, S. (2011). IKKε regulates cell elongation through recycling endosome shuttling. *Dev. Cell* **20**, 219-232.
Pokrywka, N. J. and Stephenson, E. C. (1995). Microtubules are a general component of mRNA localization systems in *Drosophila* oocytes. *Dev. Biol.* **167**, 363-370.
Queenan, A. M., Barcelo, G., Van Buskirk, C. and Schupbach, T. (1999). The transmembrane region of Gurken is not required for biological activity, but is necessary for transport to the oocyte membrane in *Drosophila*. *Mech. Dev.* **89**, 35-42.
Roth, S., Neuman-Silberberg, F. S., Barcelo, G. and Schüpbach, T. (1995). *cornichon* and the EGF receptor signaling process are necessary for both anteriorposterior and dorsal-ventral pattern formation in *Drosophila*. *Cell* **81**, 967-978.
Ruohola-Baker, H., Jan, L. Y. and Jan, Y. N. (1994). The role of gene cassettes in axis formation during *Drosophila* oogenesis. *Trends Genet.* **10**, 89-94.
Schüpbach, T. (1987). Germ line and soma cooperate during oogenesis to establish the dorsoventral pattern of egg shell and embryo in *Drosophila melanogaster*. *Cell* **49**, 699-707.
Shapiro, R. S. and Anderson, K. V. (2006). *Drosophila* Ik2, a member of the IκB kinase family, is required for mRNA localization during oogenesis. *Development* **133**, 1467-1475.
Snee, M. J. and Macdonald, P. M. (2009). Bicaudal C and trailer hitch have similar roles in gurken mRNA localization and cytoskeletal organization *Dev. Biol.* **328**, 434-444.
Somma, M. P., Ceprani, F., Bucciarelli, E., Naim, V., De Arcangelis, V., Piergentili, R., Palena, A., Ciapponi, L., Giansanti, M. G., Pellacani, C. et al. (2008). Identification of *Drosophila* mitotic genes by combining co-expression analysis and RNA interference. *PLoS Genet.* **4**, e1000126.
Spradling, A. C. and Rubin, G. M. (1982). Transposition of cloned P elements into *Drosophila* germ line chromosomes. *Science* **218**, 341-347.
St Johnston, D. and Nüsslein-Volhard, C. (1992). The origin of pattern and polarity in the *Drosophila* embryo. *Cell* **68**, 201-219.
Swan, A. and Suter, B. (1996). Role of Bicaudal-D in patterning the *Drosophila* egg chamber in midoogenesis. *Development* **122**, 3577-3586.
Theurkauf, W. E. (1994). Microtubules and cytoplasm organization during *Drosophila* oogenesis. *Dev. Biol.* **165**, 352-360.
Vanzo, N. F. and Ephrussi, A. (2002). Oskar anchoring restricts pole plasm formation to the posterior of the *Drosophila* oocyte. *Development* **129**, 3705-3714.
Weil, T. T., Forrest, K. M. and Gavis, E. R. (2006). Localization of bicoid mRNA in late oocytes is maintained by continual active transport. *Dev. Cell* **11**, 251-226.
Weil, T. T., Parton, R., Davis, I. and Gavis, E. R. (2008). Changes in bicoid mRNA anchoring highlight conserved mechanisms during the oocyte-to-embryo transition. *Curr. Biol.* **18**, 1055-1061.
Wilhelm, J. E., Buszczak, M. and Sayles, S. (2005). Efficient protein trafficking requires trailer hitch, a component of a ribonucleoprotein complex localized to the ER in *Drosophila*. *Dev. Cell* **9**, 675-685.
Zimyanin, V. L., Belaya, K., Pecreaux, J., Gilchrist, M. J., Clark, A., Davis, I. and St Johnston, D. (2008). In vivo imaging of oskar mRNA transport reveals the mechanism of posterior localization. *Cell* **134**, 843-853.